Nanoscale superconducting-gap variations and lack of phase separation in optimally doped $BaFe_{1.86}Co_{0.14}As_2$

F. Massee,[*] Y. Huang, R. Huisman, S. de Jong, J. B. Goedkoop, and M. S. Golden

Van der Waals–Zeeman Institute, University of Amsterdam, 1018XE Amsterdam, The Netherlands

(Received 8 April 2009; revised manuscript received 20 May 2009; published 30 June 2009)

We present tunneling data from superconducting $BaFe_{1.86}Co_{0.14}As_2$ and its parent compound, $BaFe_2As_2$. In the superconductor, clear coherencelike peaks are seen across the whole field of view, and their analysis reveals nanoscale variations in the superconducting gap value, Δ. The average peak-to-peak separation gives a 2Δ of $\sim 7.4 k_B T_c$, which exceeds the BCS weak coupling value for either *s*- or *d*-wave superconductivity. The characteristic length scales of the deviations from the average gap value and of anticorrelations observed between the gap magnitude and both the zero-bias conductance and coherence peak strength match well with the average separation between the Co dopant ions in the superconducting FeAs planes.

The pnictide high-T_c superconductors,[1] with maximal T_c's currently exceeding 55 K,[2] are the subject of global scrutiny on a level at par with that seen for the cuprates. One of the most debated issues are their similarities and differences with respect to the cuprates.[3] The pnictides display many features that we recognize from the cuprate repertoire, yet there are arguments that they are essentially different.[4] In the last few years, scanning tunneling microscopy and spectroscopy (STM/STS) have played a major role in investigating the electronic structure of the cuprates on length scales down to those of the atom.[5–9] This effort has brought the role of intrinsic disorder introduced by dopant atoms into sharp focus. Consequently, $BaFe_{2-x}Co_xAs_2$ is of great interest not only as an electron-doped pnictide but also because the electronically active dopants in this system are situated in the superconducting layers themselves.

Single crystals of superconducting $BaFe_{1.86}Co_{0.14}As_2$ and the nonsuperconducting parent compound $BaFe_2As_2$ (Ba122) were grown using a self-flux method. Typical crystal sizes are $1 \times 1 \times 0.1$ mm^3 [see Fig. 1(b)]. The high quality of our crystals is illustrated in Fig. 1(a), with the parent compound displaying the well-known resistivity kink at 130 K, which has been associated with a spin-density wave and accompanying orthorhombic phase transition.[10–13] Co doping erases any sign of these transitions in the resistivity but brings with it a very sharp transition into the superconducting state, which takes place at 22 ± 0.25 K in this case.

For the STM investigation, crystals were cleaved at a pressure of 5×10^{-10} mbar at room temperature in a preparation chamber and were immediately transferred into the STM chamber (base pressure $< 1.5 \times 10^{-11}$ mbar), where they were cooled to 4.2 K. The experiments were carried out using electrochemically etched W and cut Pt/Ir tips, which were conditioned before each measurement on a Au(778) single crystal and yielded identical results. In all cases, the spectral shapes obtained were independent of the tip to sample distance.[14]

Low-energy electron diffraction (LEED) was performed *in situ*, directly after the STM/STS measurements. For all measured samples, only the tetragonal unit cell spots were seen in LEED [see Fig. 2(a)], with no sign of extra spots (or extinctions) as would occur as a result of a significant and structurally coherent reconstruction of the atomic positions at the surface.

We begin our discussion with the Co-doped crystals. A constant current image with atomic resolution is shown in Fig. 2(a). In general, over areas of up to 150×150 nm^2, we saw no sign of steps on the surface, with the maximal apparent corrugation being less than 1.5 Å on all the data shown here.

From the zooms shown in Figs. 2(b) and 2(c), one can immediately see that the surface atoms lie arranged along the direction of the clear (1×1) tetragonal unit cell we measure using LEED but that the inter-atomic spacing is quite irregular. The most frequent separation seen is ~ 8 Å, twice the tetragonal unit cell. Occasionally a row of atoms with a separation of 3.9 Å occurs, as seen in panel (c), and sometimes, the (bright) atoms sit on a black background. The irregularity in interatomic distances is reflected in the Fourier transform shown in Fig. 2(d) in which smeared-out features predominate, corresponding to a real-space separation of ~ 8 Å (marked with an 'X' on the FFT). The tetragonal lattice is barely visible in the form of weak spots, highlighted in Fig. 2(d) with a yellow arrow.

Inspection of the crystal structure of Ba122 leads to the supposition that cleavage occurs at the As-Ba interface. In order to avoid creation of a polar surface, the charge of the
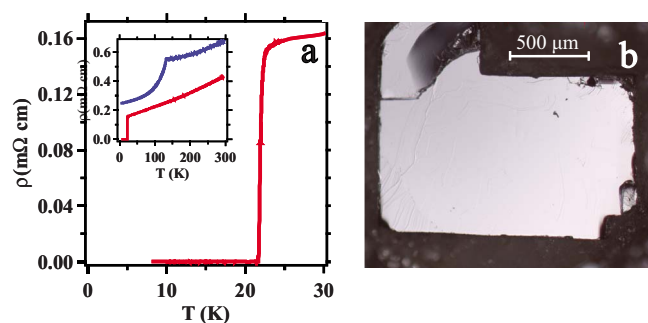
FIG. 1. (Color online) (a) Co-doped Ba122 shows a sharp superconducting transition ($\Delta T_c \sim 0.5$ K) at 22 K (red curves). The inset displays the full temperature range, with data from the parent compound (top trace). (b) Optical micrograph of the very flat cleavage surface typically obtained.
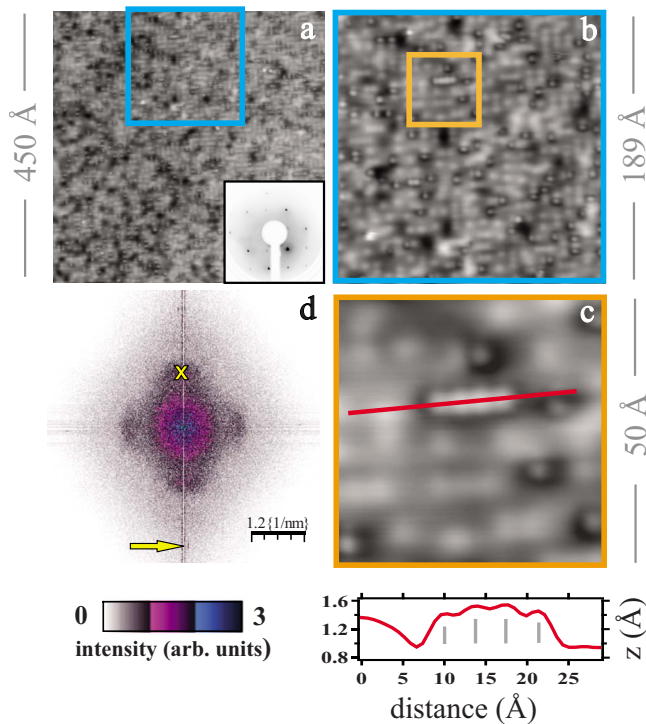
FIG. 2. (Color online) (a) Constant current image ($V_{sample}=$ -35 mV,$I_{setup}=40$ pA) of Co-doped Ba122. The inset shows LEED from the same surface with $E_0=114$ eV. (b) Zoom of panel (a): the surface atoms can be seen as bright dots. (c) Further zoom of (b) showing a row of four surface atoms separated by the tetragonal cell dimension of 3.9 Å. (d) Fourier transform of panel (a), whereby the yellow X and arrow indicate real-space distances of 8 and 3.9 Å, respectively. All data (with exception of the LEED) were recorded at 4.2 K.

FIG. 3. (Color online) (a) Constant current image from a different sample of $BaFe_{1.86}Co_{0.14}As_2$ ($V_{sample}=-88$ mV,$I_{setup}=40$ pA). (b) Analogous topography from $BaFe_2As_2$ ($V_{sample}=$ -100 mV,$I_{setup}=33$ pA). (c) Line scans from the superconducting (top) and parent (bottom) compounds taken along the arrows. Typical distances between the bright rows in the images is 12 Å indicated by gray ticks in the line scans. (d) Overlay of 400 dI/dV conductance spectra from pristine Ba122, together with their average (bold line). All data were recorded at 4.2 K.

termination layer of a system such as the pnictides should be $-1/2$ of that of the layer beneath,[4] and this condition can be met in Ba122 if exactly half of the Ba atoms remains on each of the surfaces created by cleavage. For a room-temperature cleave, the Ba ions may reorder to minimize their mutual Coulomb repulsion, resulting in interatomic distances larger that the in-plane tetragonal lattice constant, as seen in Fig. 2.

Although the LEED patterns from all studied surfaces after room-temperature cleavage show a nonreconstructed (1×1) tetragonal pattern, on an STM length scale, the details of the topography vary from cleave to cleave and occasionally also for different locations on the same cleave. A commonly encountered variation is shown in Fig. 3(a) from a different Co-doped crystal of the same doping level in which the atomic contrast is absent, and a two-dimensional (2D), mazelike network is seen, oriented along the tetragonal axes with typical period of ~12 Å. This image resembles previously reported one-dimensional stripelike structures,[15,16] whereby our "stripes" appear cut into shorter and more disordered segments, probably as a result of the higher cleavage temperature. This is in keeping with a recent report of a temperature dependence of the surface topology in a related system.[17] In Fig. 3(b), we show an image from pristine Ba122, which displays a very similar surface topology as in panel (a), as can also be seen from the line scans through both images shown in panel (c).

We now move on to the tunneling spectra. Differential conductance spectra (dI/dV) of both the Co-doped and pristine Ba122 systems were recorded (modulation amplitude of 2mV at a lock-in frequency of 427.3 Hz) on a square 64×64 pixel grid at 4.2 K. The spectra for the Co-doped system vary significantly between different locations within a single field of view (FOV).

In Fig. 4(a) we plot representative STS spectra for differing gap values (each spectrum is an average of four adjacent pixels). The spectra show not only a clear variation in peak-to-peak separation, hereafter taken as a measure of the superconducting gap (2Δ), but also in the value of the conductance at zero bias (ZBC) and in the strength of the coherence peaks. They also vary in their asymmetry and in the form of the higher-energy structures. While these latter variations are more pronounced than those reported in Ref. 16, they are less dramatic than observed in a study of the related $Sr_{1-x}K_xFe_2As_2$ compound.[15] Naturally, we are interested in the real-space 2Δ distribution and thus plot the peak-to-peak separation from all 4096 spectra as a gap map in Fig. 4(b). The map indicates that the major part of the FOV supports a gap, Δ, of 7 meV, with smaller patches of dimension between 5 and 10 Å possessing significantly smaller (darker) and larger (brighter) gaps. From this FOV, only a handful of spectra did not exhibit coherencelike peaks, and thus if these peaked structures give the superconducting gap, we can exclude phase separation between superconducting and nonsuperconducting (magnetic) regions from these data.

From Figs. 4(a) and 4(b) it is clear that $BaFe_{1.86}Co_{0.14}As_2$ supports $2\Delta/k_BT_c$ values between 5.3 for the smaller gaps, through 7.4 for the modal gap value (7 meV) to 10.6 for the largest gaps. Our modal gap is close to that seen recently in angle resolved photoemission spectroscopy (ARPES) from optimally Co-doped Ba122 for the outermost Γ centered (Γ_2 or β) Fermi surface[18] and is in keeping with data from an-
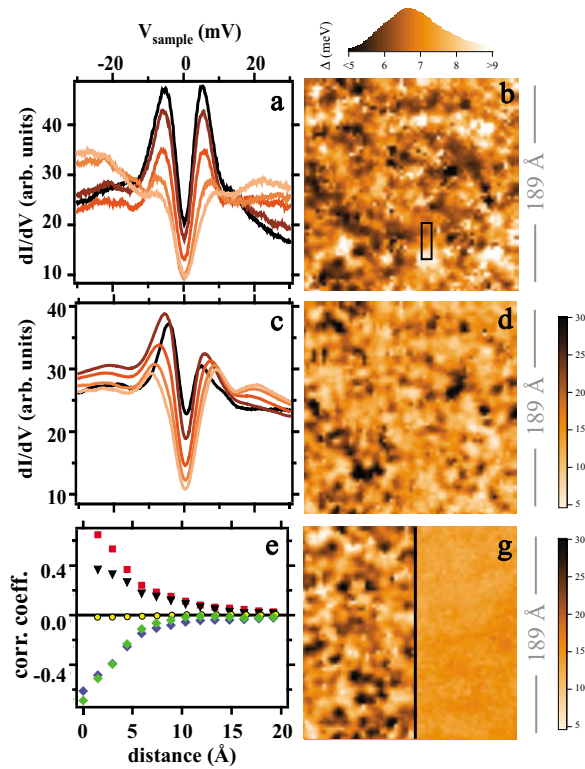
FIG. 4. (Color online) (a) STS spectra from $BaFe_{1.86}Co_{0.14}As_2$ (averages of four adjacent pixels) displaying different values of Δ, taken from the region marked in panel (b). (b) Gap map with identical FOV as Fig. 2(b), taken with the same setup conditions. (c) Binned spectra for five ranges of Δ (Ref. 20), plotted in colors matching those in the gap map. (d) Map of the zero-bias conductance on an inverted color scale from the same data set as panel (b). (e) Correlation functions. From top to bottom: autocorrelation of the gap map shown in panel (b) (red squares) and of an analogous data set recorded from the FOV shown in Fig. 3(a) (black triangles). Yellow dots: cross correlation of the gap map of panel (b) with the corresponding topograph [Fig. 2(b)]. Blue (green) diamonds: cross correlations between the gap and ZBC (peak-strength) maps. (f) Map of the coherence peak strength [for half of the FOV of panels (b) and (d), and on an inverted color scale], extracted from a comparison of the coherence peak weight to the high energy background. (g) ZBC map of pristine Ba122 recorded from half the FOV shown in Fig. 3(b). The conductance scale (shown on the right) is the same as that used in panel (d).

other STS experiment on Co-doped Ba122.[16] We also note that our normalized gap values are in line with ARPES data from the outer hole pocket Fermi surface in hole-doped (Ba,K)-122 system.[19] At present it is unclear whether the STS tunneling matrix elements favor the hole or electron pocket Fermi surfaces, but in any case, all of the normalized gap values we observe are greater than those expected for a weakly coupled BCS s- or d-wave superconductor.

Closer inspection of Fig. 4(a) reveals a relation among the ZBC, 2Δ, and the coherence peak strength: when 2Δ is small (large), the ZBC is large (small), and the coherence peaks are strong (weak). To see whether these relations hold for the whole data set, we conduct three qualitative tests. First, we plot in Fig. 4(c) the results of binning all the STS spectra into five groups, depending on their peak-to-peak separation.[20]

Second, we show in Fig. 4(d) a map of the ZBC value, with an inverted color scale to ease comparison with panel (a). Third, we map the spatial distribution of the coherence peak strength for this sample [Fig. 4(f)] and note that this gives a nearly identical image to the ZBC map in panel (d). The fact that the inverse relation between 2Δ and ZBC (and between 2Δ and the coherence peak strength) is also clearly visible in the binned (i.e., highly averaged) STS spectra and the fact that the gap, ZBC and peak strength maps resemble each other closely (providing the color scale in the latter two maps is inverted) indeed indicate that the relation among 2Δ, ZBC, and peak strength holds for the data set as a whole and not just for the STS spectra shown in Fig. 4(a).

In a next step, we formalize the relations between the $2\Delta \Leftrightarrow$ ZBC and peak-strength maps by comparing their azimuthal-integrated cross correlation traces. Figure 4(e) shows the results, indicating a clear anticorrelation that dies off over $8-10$ Å. The question arises as to the origin of the observed spatial disorder in the 2Δ values. As a first suspect, we consider the nontrivial surface topography illustrated in Figs. 2 and 3. Here, pristine Ba122 offers the best test of this point as it possesses the same complex Ba termination topography and yet is void of substitutional disorder within the FeAs structural unit. Figure 3(d) shows a compilation of one-tenth of a complete STS data set (400 of 4096 STS spectra) and their average—taken from pristine Ba122 across the same FOV as the topograph shown in Fig. 3(b). The near-E_F electronic states in the parent compound are fairly spatially homogeneous in terms of both the shape of the spectra and the absolute dI/dV value.

To compare the variation in absolute conductance with that seen in the superconductor, we show a ZBC map from pristine Ba122 in Fig. 4(g), using the same color scale as Fig. 4(d), after correction for the difference in junction resistance. Although the two ZBC maps are from different cleaves of differing materials, it is still obvious that the pristine material has much less variation and does not possess structure on the length scales of the superconductor. Thus, the gap disorder seen in Fig. 4 is a property of the superconducting system, and the finger is quickly pointed in the direction of the Co dopants as the culprit. For our doping level, 1 in 14 Fe atoms is replaced by a Co dopant, and at a zeroth level this gives a Co-Co separation of a little over 10 Å. The first length scale over which Co disorder would be visible is therefore 10 Å, as observed here. In Fig. 4(e) we show autocorrelation traces for the gap map in Fig. 4(b) and the analogous trace for a gap map recorded from an identical FOV as Fig. 3(a), i.e., a superconductor cleave with a clearly different topography yet similar STS spectra. Both these (positive) correlation traces show that 8 Å is the characteristic length scale of the significant gap variations, which is very close to the Co-Co length scale. The fact that the atomically resolved cleaves [Fig. 2(a)] and those with the 2D mazelike structure (Fig. 3(a)) both give the same length scales for the deviations from 2Δ is a further indication that in these cases the topographic details—which most likely track the particulars of the surface Ba (dis)order—do not have much direct effect on the superconducting system. We note that—albeit on a somewhat coarser energy scale—similar conclusions have been drawn from a recent photoemission study of the Ba122

system.[21] Finally, we remark that the cross correlation traces between the gap map and the topography are zero for both types of topography [see Fig. 4(e)].

How do the spatial gap variations found here in an electron doped pnictide compare with those from STS studies of the cuprate high T_c's at analogous doping levels? Optimally doped Bi2212 yields a similar total spread of a factor of 2 in normalized gap values but upshifted with respect to those here to lie between 6 and $13k_BT_c$.[7] Recently, the emphasis has come to lie on the role played by the pseudogap in the observed large apparent superconducting gap disorder seen in the cuprates.[22] In the pnictide STS data presented here, it would be natural to take the modal gap value as that representing areas with Co doping occurring in the FeAs plane at the nominal level. Consequently, the small gaps could either be under- or overdoped regions formed due to clustering of Co since both would—in principle—lead to a lower T_c (and presumably Δ). This would leave only the larger peak-to-peak separations unaccounted for. To decide whether, as in the cuprates, these large-gap regions are related to the presence of a pseudogap or not will require detailed temperature-dependent measurements.

In summary, we present detailed STM and STS investigations of pristine Ba122 and samples of the electron doped superconductor $BaFe_{1.86}Co_{0.14}As_2$. In the first part of the Rapid Communication we describe the complex topography

of the surfaces of these single crystals, which is probably a result of partial liftoff of the Ba ions upon cleavage. We go on to demonstrate that the termination-plane topographic disorder encountered here has little effect on the low-lying electronic states of these systems.

The STS data from the superconducting samples display clear coherence-peak-like features defining an energy gap of on average $7.4k_BT_c$. There exist, however, significant spatial deviations from this modal gap value, with the gap distribution ranging from $5-10k_BT_c$. If these gaps are indeed superconducting gaps, we can clearly rule out nanoscopic phase separation in these samples. There is a robust anticorrelation between the peak-to-peak separation and the zero-bias conductance, and coherence peak strength, operating over length scales of ~ 8 Å. The spatial correlation of the low and high gap deviations from the modal gap value also displays the same length scale, one which is very close to the average separation of the Co atoms in the FeAs superconducting blocks, highlighting their importance as local dopants.

*f.massee@uva.nl

[1] Y. Kamihara, T. Watanabe, M. Hirano, and H. Hosono, J. Am. Chem. Soc. **130**, 3296 (2008).

[2] Z.-A. Ren, G.-C. Che, X.-L. Dong, J. Yang, W. Lu, W. Yi, X.-L. Shen, Z.-C. Li, L.-L. Sun, F. Zhou, and Z.-X. Zhao, Chin. Phys. Lett. **25**, 2215 (2008).

[3] M. R. Norman, Physics **1**, 21 (2008).

[4] G. Sawatzky, I. Elfimov, J. van den Brink, and J. Zaanen, arXiv:0808.1390 (unpublished).

[5] Ø. Fischer, M. Kugler, I. Maggio-Aprile, and C. Berthod, Rev. Mod. Phys. **79**, 353 (2007).

[6] S. H. Pan, E. W. Hudson, K. M. Lang, H. Eisaki, S. Uchida, and J. C. Davis, Nature (London) **403**, 746 (2000).

[7] K. McElroy, R. W. Simmonds, J. E. Hoffman, D.-H. Lee, J. Orenstein, H. Eisaki, S. Uchida, and J. C. Davis, Nature (London) **422**, 592 (2003).

[8] J. E. Hoffman, K. McElroy, D.-H. Lee, K. M. Lang, H. Eisaki, S. Uchida, and J. C. Davis, Science **297**, 1148 (2002).

[9] K. K. Gomes, A. N. Pasupathy, A. Pushp, S. Ono, Y. Ando, and A. Yazdani, Nature (London) **447**, 569 (2007).

[10] M. Rotter, M. Tegel, D. Johrendt, I. Schellenberg, W. Hermes, and R. Pöttgen, Phys. Rev. B **78**, 020503(R) (2008).

[11] J. Dong, H. J. Zhang, G. Xu, Z. Li, G. Li, W. Z. Hu, D. Wu, G. F. Chen, X. Dai, J. L. Luo, Z. Fang, and N. L. Wang, EPL **83**, 27006 (2008).

[12] T. Nomura, S. W. Kim, Y. Kamihara, M. Hirano, P. V. Sushko, K. Kato, M. Takata, A. L. Shluger, and H. Hosono, Supercond. Sci.

Technol. **21**, 125028 (2008).

[13] G. F. Chen, Z. Li, D. Wu, G. Li, W. Z. Hu, J. Dong, P. Zheng, J. L. Luo, and N. L. Wang, Phys. Rev. Lett. **100**, 247002 (2008).

[14] C. Renner and Ø. Fischer, Phys. Rev. B **51**, 9208 (1995).

[15] M. Boyer, K. Chatterjee, W. Wise, G. Chen, J. Luo, N. Wang, and E. Hudson, arXiv:0806.4400 (unpublished).

[16] Y. Yin, M. Zech, T. L. Williams, X. F. Wang, G. Wu, X. H. Chen, and J. E. Hoffman, Phys. Rev. Lett. **102**, 097002 (2009).

[17] D. Hsieh, Y. Xia, L. Wray, D. Qian, K. Gomes, A. Yazdani, G. Chen, J. Luo, N. Wang, and M. Hasan, arXiv:0812.2289 (unpublished).

[18] K. Terashima, Y. Sekiba, J. H. Bowen, K. Nakayama, T. Kawahara, T. Sato, P. Richard, Y.-M. Xu, L. J. Li, G. H. Cao, Z.-A. Xu, H. Ding, and T. Takahashi, Proc. Natl. Acad. Sci. U.S.A. **106**, 7330 (2009).

[19] L. Wray, D. Qian, D. Hsieh, Y. Xia, L. Li, J. Checkelsky, A. Pasupathy, K. Gomes, A. Fedorov, G. Chen, J. Luo, A. Yazdani, N. Ong, N. Wang, and M. Hasan, Phys. Rev. B **78**, 184508 (2008).

[20] Δ values have been binned as follows: 0–5.5, 5.5–6.5, 6.5–7.5, 7.5–8.5, 8.5-Δ_{max} meV.

[21] S. de Jong, Y. Huang, R. Huisman, F. Massee, S. Thirupathaiah, M. Gorgoi, F. Schaefers, R. Follath, J. B. Goedkoop, and M. S. Golden, Phys. Rev. B **79**, 115125 (2009).

[22] M. C. Boyer, W. D. Wise, K. Chatterjee, M. Yi, T. Kondo, T. Takeuchi, H. Ikuta, and E. W. Hudson, Nat. Phys. **3**, 802 (2007).